

ASSESSING ROLES OF VOLCANISM AND BASIN SUBSIDENCE IN CAUSING OLIGOCENE–LOWER MIOCENE SEDIMENTATION IN THE NORTHERN RIO GRANDE RIFT, NEW MEXICO, U.S.A.

GARY A. SMITH¹, JESSICA D. MOORE^{1*}, AND WILLIAM C. MCINTOSH²

¹ Department of Earth and Planetary Sciences, University of New Mexico, Albuquerque, New Mexico 87131, U.S.A.

² New Mexico Bureau of Geology and Mineral Resources, 801 Leroy Place, Socorro, New Mexico 87801, U.S.A.

ABSTRACT: Oligocene, mostly volcanoclastic, fluvial sedimentation in the Rio Grande rift of northern New Mexico has been ascribed to either aggradation in response to explosive volcanism or initial subsidence of extensional basins. These competing interpretations are tested by numerical simulations and by stratigraphic and petrographic study of the Oligocene–lower Miocene Abiquiu Formation. The upper 450 m of the > 600-m-thick Abiquiu Formation is tuffaceous volcanoclastic sediment that accumulated during explosive volcanic activity in the Latir volcanic field, about 150 km to the northeast. The formation extends westward beyond the most conspicuous rift-bounding faults. Simple numerical simulations suggest that two volcanism-related processes may have contributed to sedimentation. First, stream longitudinal profiles adjust upward as a result of (a) increasing headwater elevation in volcanic constructional topography and (b) increased sediment load. These combined effects may produce as much as 100 m of deposition at distances in excess of 150 km from the volcanic source area. The second volcanic mechanism is flexural subsidence resulting from the load of volcanic fields and flanking volcanoclastic aprons, and may account for 300 m or more preservation space at a distance of 150 km. Correlation of stratigraphic intervals of the Abiquiu Formation defined by lithofacies geometry and sandstone composition reveals thickening of strata into the rift across rift-bounding and intra-rift faults, indicating subsidence-driven sedimentation. Petrographic and ⁴⁰Ar/³⁹Ar geochronologic data reveal that sediment was derived mostly or wholly from ignimbrites erupted in the Latir volcanic field, including widespread deposition of pumiceous debris-flow deposits following emplacement of the 25.1 Ma Amalia Tuff. Deposition of the Abiquiu Formation was therefore most likely caused by a combination of rift-basin subsidence and volcanism-related isostatic subsidence and adjustments of stream profiles.

INTRODUCTION

Preservation of nonmarine sediment in continent interiors is driven largely by basin subsidence. With sufficient sediment supply, streams tend to infill subsiding basins to maintain graded longitudinal profiles and produce successions that may be many kilometers thick. Volcanism is an additional influence wherein modest (hundreds of meters), long-term aggradation is caused by regrading of rivers inundated by large volumes of volcanoclastic debris (Smith 1987, 1991). Because volcanism and basin subsidence occur simultaneously in many tectonically active regions, it is desirable in a complete basin analysis to distinguish these two driving forces for sediment accumulation and preservation (*sensu* Blum and Törnqvist 2000).

The relative roles of subsidence-driven and volcanism-driven sedimentation are the focus of controversy over the time of initiation of the Rio Grande rift in northern New Mexico (Fig. 1). Extension in this area is traditionally viewed as beginning in the late Oligocene on the basis of (1) stratigraphic and subsurface data indicating basin-floor tilting in southern Colorado and (2) the inference that widespread basaltic volcanism beginning at 25–27 Ma heralded lithosphere extension (Lipman and Mehnert 1975; Lipman 1983; Baldrige et al. 1980; Chapin 1988; Brister and Gries

1994; Chapin and Cather 1994). Ingersoll et al. (1990) and Large and Ingersoll (1997) point out that very little is known about the extent of faulting and associated tilting of rift-basin-fill sediment during the late Oligocene and early Miocene and attribute the best-documented deformation, in close proximity to magmatic centers, to local strain associated with thermal weakening of the crust. Oligocene, primarily volcanoclastic, sedimentation in northern New Mexico clearly persisted beyond the rift boundaries (Figs. 1, 2), further suggesting the lack of distinct rift-bounding faults at that time (Baltz 1978; Morgan and Golombek 1984). Ingersoll et al. (1990) suggest that widespread Oligocene volcanoclastic-sediment aprons aggraded in response to volcanism in adjacent volcanic fields and are not indicative of rift-basin formation, which may not have begun until after 21 Ma (Large and Ingersoll 1997). Baldrige et al. (1994) suggest that subsidence of the Abiquiu embayment (Figs. 1, 2), the focus of this study, occurred in the short interval between 10 Ma and 7 Ma following accumulation of 1.1 km of mostly volcanoclastic alluvium.

The objectives of this paper are to provide (1) a semiquantitative assessment of volcanism-driven aggradation and (2) to examine stratigraphic evidence for syndepositional basin subsidence in the southwestern Abiquiu embayment of the Rio Grande rift. The approaches and results of these two independent studies are reported separately and then integrated. This effort was undertaken not only to resolve controversy over the age of rift initiation in northern New Mexico but also to provide insights applicable to separating volcanic and tectonic-subsidence signals in other continental-interior basins.

GEOLOGIC SETTING

The Abiquiu embayment is a structurally shallow bench along the western margin of the Rio Grande rift in northern New Mexico (Fig. 1). The embayment contains approximately 1.1–1.5 km of Oligocene and Miocene sedimentary and volcanic fill adjacent to the deeper east-tilted San Luis basin half graben and west-tilted Española basin half graben, each of which contain more than 5 km of basin fill (Fig. 1; Kelley 1978; Smith in press). Basement-cored uplifts of the Late Cretaceous–early Tertiary Laramide orogeny form the Tusas Mountains and Sierra Nacimiento on the north and southwest sides of the embayment, respectively, and sedimentary fill of the embayment is concealed beneath the younger Jemez Mountains volcanic field to the south (Fig. 1). Most of the western embayment margin exists as discrete faults separating Oligocene–Miocene strata from upper Paleozoic through lower Tertiary rocks of the Colorado Plateau (Fig. 1). Erosional remnants of Oligocene and Miocene sedimentary rocks, locally capped by upper Miocene basalt flows, are found west of these faults, most notably at Cerro Pedernal (Figs. 1, 2) and in the northern Sierra Nacimiento. Basin-filling strata within the Abiquiu embayment thicken eastward across a series of steeply east-dipping normal faults (Kelley 1978; Baldrige et al. 1994) such that the oldest sediment is exposed only in the westernmost fault blocks (Figs. 1, 2; Kelley 1978). Deformation of pre-Tertiary rock along the Cañones fault and southwestward thickening of syn-Laramide strata of the El Rito Formation (Fig. 2) across the fault imply that this structure, and possibly intrabasinal faults, were west-vergent oblique-reverse faults during the Laramide deformation (Moore 2000). Bedding attitudes in Oligo–Miocene rocks within the embayment are variable (Kelley 1978; May 1980), but dips in sedimentary strata are mainly to the southwest within the western embayment study area (Fig. 2; Moore

* Present Address: ExxonMobil Exploration Company, 222 Benmar, Houston, Texas 77060, U.S.A.

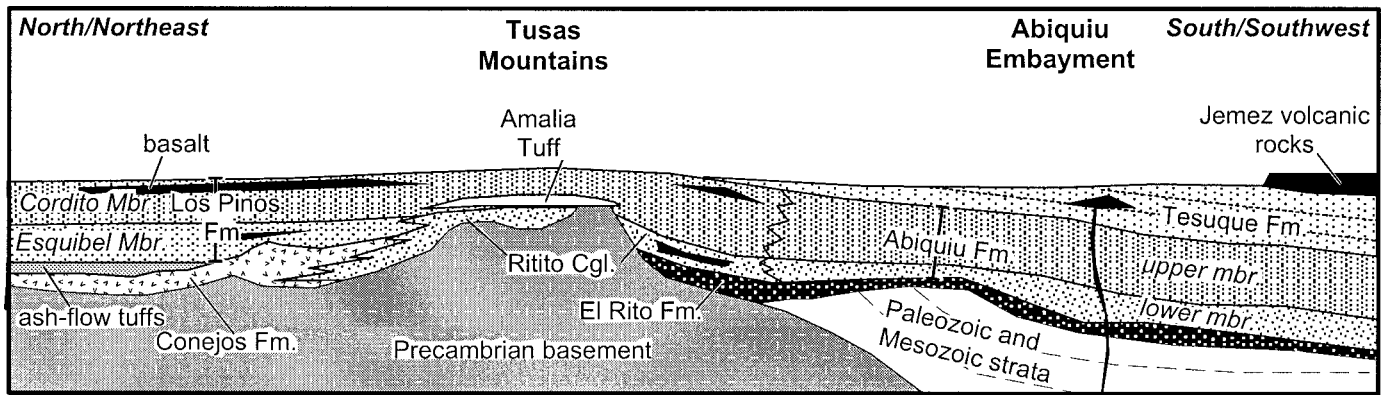


Fig. 3.—Regional stratigraphic relationships emphasizing correlations between the Tusas Mountains and Abiquiu embayment. Diagram is not drawn to scale and is very schematic (modified from Manley 1981).

2000). Miocene (~ 10–7.6 Ma; Baldrige et al. 1994) basalt flows rest unconformably on top of the sedimentary basin fill and preserve northward depositional gradients away from the Jemez Mountains.

The Oligocene–lower Miocene sedimentary rocks in the Tusas Mountains and Abiquiu embayment are derived primarily from coeval volcanic fields to the north and northeast. In the study area, these volcanoclastic strata are as much as 450 m thick (Moore 2000) and form the upper member of the Abiquiu Formation (Fig. 3; Vazzana and Ingersoll 1981; Ingersoll and Cavazza 1991). The lower member of the Abiquiu Formation is a c. 30–125 m thick conglomerate derived almost entirely from Precambrian crystalline rock (Smith 1938; Vazzana 1980; Moore 2000). The locally intervening Pederal chert member consists of calcite- and chalcedony-cemented ledges within mostly nonvolcanoclastic conglomerate restricted to westernmost outcrops of the Abiquiu Formation.

Within and north of the Tusas Mountains the lower member of the Abiquiu Formation is correlative with the Ritito Conglomerate and the upper member is correlative with the Los Pinos Formation (Barker 1958; Bingle 1968; Manley 1981; Fig. 3). The Los Pinos Formation consists of the lower Esquibel Member, composed chiefly of intermediate-composition volcanic detritus, and the upper Cordito Member, which contains a greater abundance of alkali-rhyolite detritus (Barker 1958; Butler 1971; Manley 1981). Esquibel Member volcanoclastic strata and the underlying Conejos Formation (30–35 Ma; Lipman and Mehnert 1975; Lipman 1989) (Fig. 3) are derived from the San Juan volcanic field, centered in southern Colorado. The Esquibel Member overlies 31.0–28.4 Ma dacitic and quartz latitic ignimbrites of the southeast caldera cluster (Fig. 1; Lipman 1975, 1989; Lipman et al. 1996; Manley 1981; Ingersoll and Cavazza 1991). Cordito Member rhyolitic detritus is derived from the Latir volcanic field (Fig. 1; Manley 1981; Ingersoll and Cavazza 1991), now partly exposed in the Sangre de Cristo Mountains (Fig. 1), which was active between 28.4 and 18 Ma (Lipman 1983; Ingersoll and Cavazza 1991; Bauer et al. 1999), and contains the 25.1 Ma Amalia Tuff (new age data reported herein). The volcanic record of the Latir volcanic field following eruption of the Amalia Tuff comes mostly from dated sedimentary clasts (Ekas et al. 1984; Ingersoll and Cavazza 1991; Moore 2000) or is inferred from dated plutons because volcanic rocks were subsequently largely eroded from uplifted parts of the Latir field in the Sangre de Cristo Mountains or buried beneath younger fill of the San Luis Basin (Smith in press). Basalt flows with K–Ar ages mostly between 28 Ma and 17 Ma are found within the Los Pinos Formation and Ritito Conglomerate (Lipman and Mehnert 1975, 1979; Baldrige et al. 1980). The Abiquiu and Los Pinos Formations are overlain by distinctly less tuffaceous, but still primarily volcanoclastic, strata of the Tesuque Formation and basalt from the Jemez Mountains (Fig. 3).

Knowledge of the provenance of volcanoclastic strata in the Abiquiu embayment is critical in reconstructing Oligocene paleogeography. Smith

(1938), Ingersoll et al. (1990), and Ingersoll and Cavazza (1991) interpret a San Juan volcanic field source for the upper member of the Abiquiu Formation, whereas Bingle (1968) and Manley (1981) correlate these same strata to the Latir-derived Cordito Member. Smith (1995) corroborated the presence of Cordito-like rhyolitic detritus in the Abiquiu Formation while suggesting that a San Juan source remained possible for lower parts of the upper member. The San Juan volcanic field ignimbrites and volcanoclastic-sediment apron are mostly or entirely restricted to the northeast side of the Tusas Mountains (Barker 1958; Bingle 1965, 1968; Doney 1968; Muehlberger 1967, 1968; Manley and Wobus 1982a, 1982b; Wobus and Manley 1982), which apparently formed an Eocene–Oligocene topographic barrier that was not buried until deposition of the Cordito Member (Fig. 3).

VOLCANISM-DRIVEN DEPOSITION?

Hypothesis

The highly tuffaceous nature of the upper Abiquiu Formation and Los Pinos Formation and the presence of ignimbrites within the Los Pinos Formation demonstrate deposition of these strata contemporaneously with explosive volcanism in the San Juan and Latir volcanic fields (Fig. 3). These volcanoclastic strata are found beyond the Rio Grande rift basins (Figs. 1, 2) where they underlie the highest peaks (above 3300 m above sea level) of the Tusas Mountains (Muehlberger 1968) and Sierra Nacimiento (Timmer 1976). It is reasonable to suggest, therefore, that deposition of these strata was, at least in part, independent of rift-basin subsidence and resulted directly from coeval volcanic activity.

We hypothesize that two mechanisms potentially link volcanism with sediment aggradation. First, volcanic activity in fluvial headwaters can cause upward adjustment of the longitudinal profiles of the draining streams (Fig. 4A). Pyroclastic deposits provide large volumes of readily eroded, mostly sand-size debris to fluvial systems. Streams typically lack the capacity to transport all of this sediment, causing aggradation throughout whole drainage basins (Smith 1991). Headwater elevations also increase as volcanic constructional topography is built upward. To some extent, this increase in headwater elevation is offset by fluvial incision. Overall landscape elevation does, however, increase and the filling of valleys by lava flows and ignimbrites can probably keep headwater reaches from achieving equilibrium during periods of high-volume extrusive activity. Second, growth of volcanic fields may cause flexural isostatic subsidence to accommodate flanking depositional aprons independently of true tectonic subsidence (Fig. 4B). The formation of a flexural moat adjacent to the Hawaiian Islands (Menard 1964; Watts 1978) led Smith et al. (1989) and Smith and Landis (1995) to suggest that continental-margin arcs could form basins wider than the constructional volcanic platform, which will then accommodate flanking volcanoclastic-sediment aprons. This model of basin for-

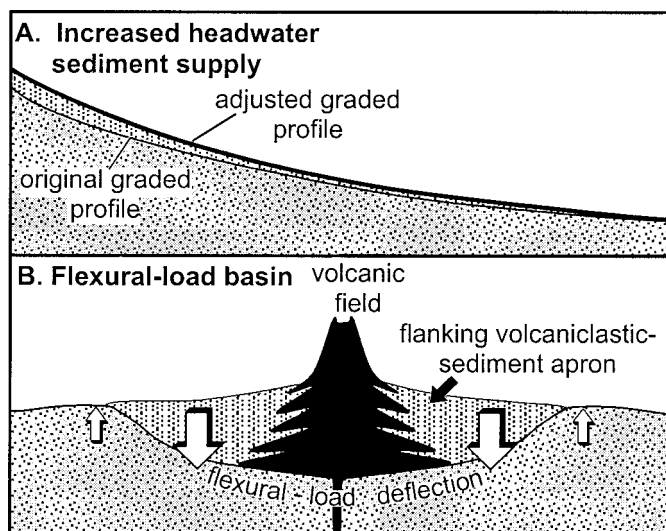


FIG. 4.—Schematic illustrations of volcanism-driven aggradation mechanisms. A) Increased sediment supply in the headwaters causes regrading of river longitudinal profiles. The area between the original and adjusted profiles represents resulting sediment aggradation, which decreases downstream. B) Vertically exaggerated representation of the flexural basin, and minor flanking forebulges, hypothesized to result from crustal loading by volcanic fields and flanking volcanoclastic-sediment aprons, partly to largely accommodated by flexural subsidence (after Smith and Landis 1995).

mation has not heretofore been examined for intracontinental volcanic fields.

Methods

The combined effects of increased sediment load and headwater elevation were evaluated by use of LONGPRO, a program that produces a two-dimensional channel profile equilibrated to a variety of channel-hydraulics and sediment parameters (Slingerland et al. 1994, chapter 7). The choice of input parameters is mostly arbitrary because detailed paleogeomorphic data are lacking. Nonetheless, we believe that order-of-magnitude estimates are reasonable and provide assessment of the validity of the hypothesis that increased load and headwater elevations raise stream profiles and cause aggradation. A 400-km-long stream profile is considered, even though the study area is ≤ 150 km from the volcanic fields, in order to avoid influences of model boundaries and because sinuosity of the depositing streams is unknown. An initial equilibrium profile was generated for a channel with

an average slope of 0.0017 and downstream water discharge of $10 \text{ m}^3/\text{s}$, values that are comparable to high-order streams draining the volcanic fields today. Longitudinal profiles were calculated for sediment-mass-feed rates between 0.5 and $1.5 \text{ m}^3/\text{s}$, Manning's- n of 0.04, and a median grain size of 1.0 mm (consistent with observations in the field; Vazzana 1980; Moore 2000). Time-varying discharge and non-point sources of sediment were not simulated. Changes in bed elevation at the various mass-feed rates represent accumulation space that is filled with sediment. Because LONGPRO uses a backwater method to calculate profile elevations, the elevation is fixed at the downstream end at an arbitrary value of 1000 m. The modeled aggradation therefore decreases downstream, consistent with the general downstream decrease in syneruption aggradation in modern river valleys (Smith 1987, 1991). The resulting increase in headwater elevation simulates the expected effect of increasing constructional relief in the volcanic field.

Flexural subsidence attributable to growth of a volcanic field was evaluated by application of CONTIN, a two-dimensional, continuous-plate flexure simulator (Slingerland et al. 1994, chapter 2). Simulated loads on the continuous plate represent all documented volcanic and vent-proximal sedimentary material in both volcanic fields (Steven et al. 1974; Lipman et al. 1996; Lipman and Reed 1989) and were adjusted upward to speculative initial heights to account for subsequent erosion (Fig. 5). Distally tapering, wedge-shaped volcanoclastic-sediment aprons were added adjacent to the simulated volcanic fields with thickness comparable to that preserved in the upper member of the Abiquiu Formation (Fig. 5). The inclusion of the volcanoclastic apron might be viewed as producing a circular argument when formulating the flexural-loading model as a means of testing whether or not the volcanic-field load can provide accommodation space for the sediment apron. Inclusion of the apron is, however, more realistic, because the flexural moat induced by the volcanic load is in all likelihood filled with sediment, which creates an additional load and increases the wavelength and amplitude of the overall flexural deflection. Rigidity values ranging from 10^{22} to 10^{24} Nm were chosen as being reasonable for a continental interior (cf. Jordan 1981). It is unknown if Oligocene magmatism was associated with sufficiently widespread heating of the crust to justify using lower values of rigidity. Because lower values decrease the wavelength of the flexural depression, our model results can be interpreted as representing the maximum distance of the influence of volcanism to induce subsidence, and therefore the resulting deflections at the distance of interest are maxima. Load densities ranging from 2250 to 2700 kg/m^3 were used to approximate variable proportions of sedimentary and volcanic rocks in the load, respectively (cf. Ahrens 1995). Variation of the density parameters by as much as 10% was found to have no significant effect on magnitude of deflection, regardless of rigidity.

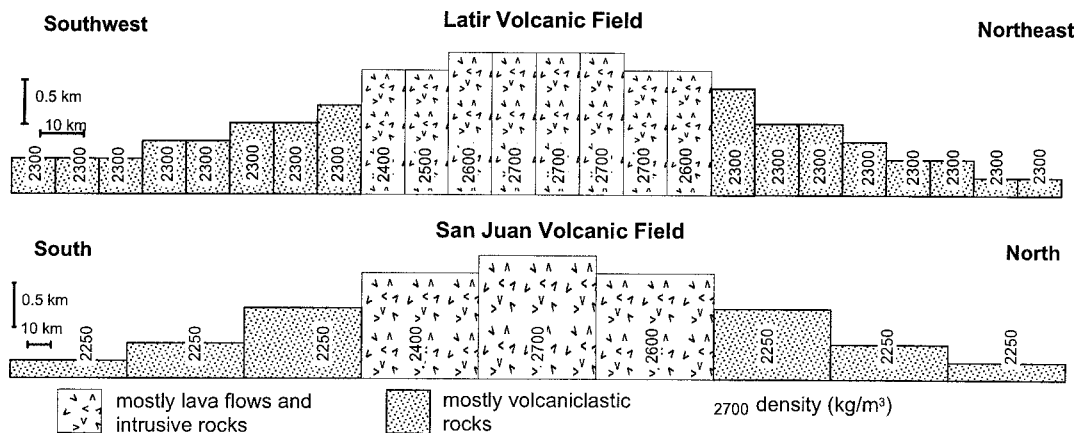


FIG. 5.—Diagrammatic representation of loads used for flexural-loading simulations of the San Juan and Latir volcanic fields.

As with the stream-profile simulations, we acknowledge that the choices of flexure-model input parameters are speculative. Principal uncertainties include the uncertain thickness and density distribution of volcanic materials within the proximal volcanic fields, the uncertain thermal state and elastic thickness of the crust during the Oligocene, the uncertain effects of hidden loads in the upper mantle and crust associated with magmatism, or the validity of a continuous-plate assumption across a complexly faulted region. Nonetheless, we suggest that these uncertainties do not inhibit a first-order assessment of the hypothesis that hundreds of meters of preservation space can arguably be created at distances of 100–200 km from a volcanic field primarily by flexure beneath the accumulating volcanic pile, modified and enhanced by the sediment accumulating in the resulting depression.

Results

The hypothesis that volcanism-driven, rather than rift-subsidence-driven, aggradation accounts for the preserved thickness of the upper member of the Abiquiu Formation is best tested by comparing simulation results to the thickness of the upper member outside of the rift. There is only one complete stratigraphic section of the upper member located west of principal Rio Grande rift faults, at Cerro Pedernal (Fig. 2). At this location the Abiquiu Formation is 412 m thick with 316 m of upper member present above the lower and Pedernal chert members, and is overlain by Tesuque Formation and Miocene basalt (Kelley 1978; Moore 2000). Cerro Pedernal is about 150 km from the southeast caldera cluster of the San Juan Mountains volcanic field and the center of the Latir volcanic field, so flexural-load simulation results at these distances were compared to the rock thickness. Use of these distances in the stream-longitudinal-profile results is problematic because stream-profile distance must incorporate channel sinuosity, which is not known. A notable lack of point-bar lateral-accretion surfaces from all but about 35 m of the upper member (Smith 1995; Moore 2000) suggests low channel sinuosity. Therefore, the channel-profile simulation results over the reach 150–200 km from the headwater node were used in comparison to the thickness of the Cerro Pedernal section.

LONGPRO Simulations.—The results from the LONGPRO simulations suggest that the combined effects of increasing headwater elevation and sediment load can cause modest aggradation at distances in excess of 150 km from the headwaters (Fig. 6). Assuming that the Cerro Pedernal locality is on the order of 150–200 stream kilometers from the headwaters, the adjustments in river profile are on the order of 60–100 m or less than a third of the thickness of volcanoclastic strata. Most of the upward adjustment in profile elevation is within 75 km of the headwaters. To simulate accumulation of the entire upper member at Cerro Pedernal using the selected hydraulic parameters would require raising headwater elevations by more than 1000 m, which we do not believe is justified by the regional geologic relationships.

We find this result interesting but acknowledge that it is not a particularly robust test of the hypothesis because of the simplifications of the model and the speculative choice of input parameters. Adjustment of modern streams to inundation by pyroclastic debris has included extreme complex responses of aggradation and downcutting (e.g., Smith 1987, 1991), which may or may not induce long-term changes in longitudinal profile of the sort simulated by LONGPRO. For that reason, we suspect that the simulated bed-elevation changes are maximum values.

CONTIN Simulations.—The results of the CONTIN flexural-loading simulations suggest that the weight of the growing volcanic fields and their flanking volcanoclastic aprons can cause approximately 200–400 m of crustal deflection at Cerro Pedernal, where the total Abiquiu Formation is 412 m thick (Fig. 7 and Table 1; see Moore 2000 for full results). A shallower deflection at this distance from the center of the load would result from application of a lower flexural rigidity. While acknowledging the uncertainty of some input parameters, we believe that they are reasonable and

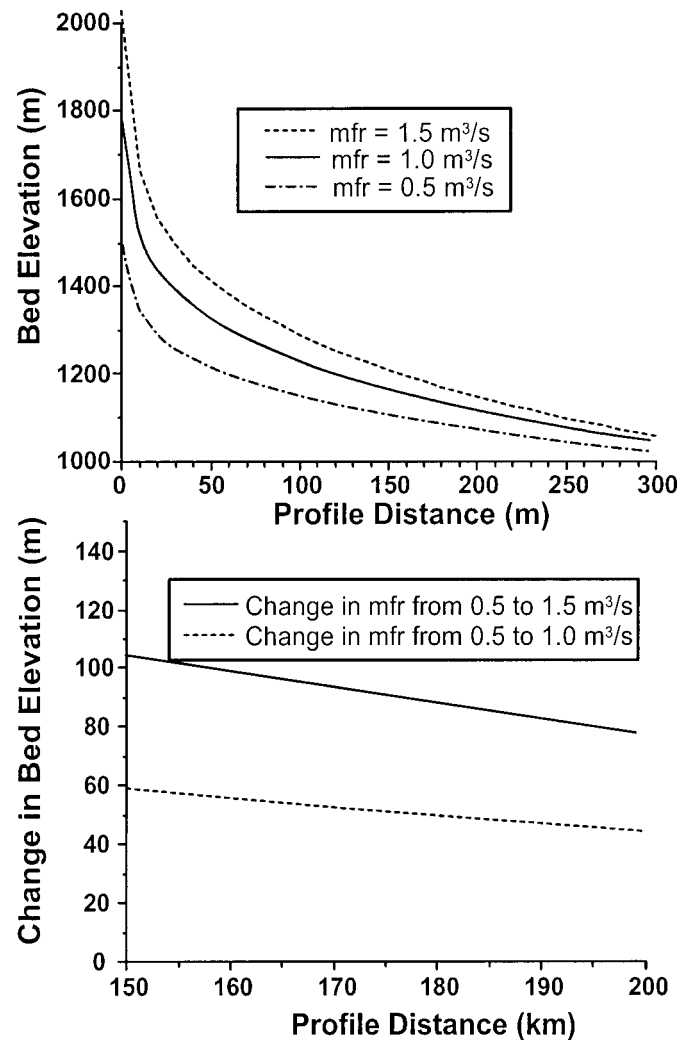


Fig. 6.—Results of LONGPRO simulations at various sediment-mass-feed rates (mfr). Upper graph: Equilibrium profiles calculated for three mass-feed rates. Lower graph: Change in bed elevation between pairs of simulations for the reach between 150 and 200 km. The change in bed elevation can be equated to the amount of aggradation that could occur because of the increase in sediment load and the ability of the headwater elevations to increase.

we are therefore confident of the implication that flexure may be an important mechanism for inducing subsidence to accommodate basin-filling sediment adjacent to volcanic fields and could account for much of the thickness of the upper member of the Abiquiu Formation at Cerro Pedernal. Of greater uncertainty is the validity of the continuous-plate flexure model where the Tusas Mountains fault block intervenes between the volcanic fields and the Abiquiu Formation outcrop belt. It is possible that deeply penetrating, frequently reactivated Proterozoic–Tertiary faults in the Tusas Mountains (Karlstrom et al. 1999; Smith in press) would inhibit transfer of load-induced stresses from the north and east to the Cerro Pedernal area.

The flexural-load results may explain the presence of nonvolcanoclastic strata in the lower Abiquiu Formation, which clearly cannot be explained by the overwhelming of streams by volcanic detritus. Stratigraphic relationships indicate that the basement-derived strata of the lower member and coeval Ritito Conglomerate south of the Tusas Mountains are temporally equivalent to San Juan–derived volcanoclastic rocks north of the Tusas Mountains (Fig. 3). Growth of the San Juan volcanic field was underway at this time and flexural subsidence could have generated preservation space south of the Tusas Mountains. Because the Tusas Mountains served as a

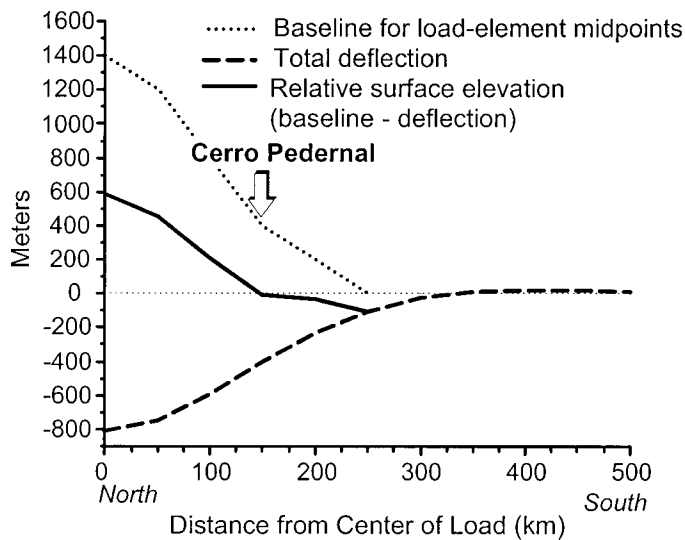


FIG. 7.—Results of CONTIN simulation with a flexural rigidity of 10^{24} Nm for a profile from the center of the San Juan volcanic field load through Cerro Pedernal. The model load (Figure 5) produces more than 400 m of deflection at the location of Cerro Pedernal.

topographic barrier to southward transport of volcanoclastic debris from the San Juan volcanic field, this shallow, distal basin was filling instead with detritus eroded from the exposed basement rocks of the Tusas Mountains and Sierra Nacimiento. The lower and Pedernal chert members of the Abiquiu Formation are 96 m thick at Cerro Pedernal (Moore 2000) giving a total thickness of 412 m for the whole formation west of the rift-bounding faults. This thickness is comparable to the maximum simulated deflection (Table 1).

Synthesis.—Computational simulations of the two hypothesized volcanism-driven aggradational mechanisms suggest that these mechanisms are sufficient to account for deposition of the upper member of the Abiquiu Formation west of the Rio Grande rift. Although simplifications in the models and uncertainty of input parameters preclude rigorous conclusion, we are satisfied with the order of magnitude of accumulation and preservation space that the model results suggest, and that they can be created under the hypothesized circumstances. Growth of volcanic fields induces flexural-load subsidence over a broad region adjacent to the magmatic region. Sediment is readily available to fill the resulting basin from the erosion of poorly consolidated volcanoclastic debris. Volcanic activity raises landscape elevation and lava flows and pyroclastic deposits fill proximal valleys, causing overall rise in the longitudinal profiles of streams, which is accommodated by downstream aggradation. The infilling of the flexurally produced basin widens the total load (Figs. 4, 5) and increases the area of subsidence by flexural compensation. Clearly, more realistic simulators and better-known input parameters are required for robust analysis, but these results suggest that aggradation of 300+ m of sediment at a distance on the order of 100–200 km from a volcanic source area is possible without

tectonically induced basin subsidence. Flexural subsidence provides more space for sediment preservation than does regrading of stream profiles in response to large sediment loads.

TECTONIC-SUBSIDENCE-DRIVEN AGGRADATION?

Hypothesis

Regionally, there is substantial evidence for Oligocene initiation of subsidence in the Rio Grande rift. Stratigraphic and subsurface data indicate eastward tilting of the San Luis basin in southern Colorado beginning at about 26–28 Ma (Lipman and Mehnert 1975; Lipman 1983; Brister and Gries 1994). Subsidence of the Española basin was possibly underway before 30 Ma (Smith 2000, in press). Widespread basaltic volcanism in the Española basin and southern San Juan Mountains volcanic field beginning at 25–27 Ma is interpreted to reveal lithosphere extension (Baldrige et al. 1980; Chapin 1988). The angular unconformity below upper Miocene basalt flows in the southwestern Abiquiu embayment (Fig. 2) suggests that basin subsidence and tilting of basin fill largely preceded the eruption of the basalts rather than being coeval with basaltic volcanism as inferred by Baldrige et al. (1994). Therefore, it is reasonable to suggest that Oligocene initiation of rift-basin subsidence in the Abiquiu embayment played a role in preserving the volcanoclastic-sediment apron represented by the upper member of the Abiquiu Formation.

If rift-basin subsidence was underway during Abiquiu Formation deposition then there should be thickening of strata from the Colorado Plateau (e.g., at Cerro Pedernal) into the Abiquiu embayment and, possibly, eastward across intrabasinal faults (Fig. 2). Because the top of the Abiquiu Formation is not preserved in most areas and the bottom is exposed only in western outcrops, it is not possible to document lateral thickness variations, if present, within the whole formation. Smith (1995) described three, lithostratigraphically distinct intervals within part of the upper Abiquiu Formation at Arroyo del Cobre (Fig. 2), which are also characterized by distinct sandstone composition indicating varying provenance. Thickness of these internal intervals should vary across faults if subsidence occurred during deposition.

Methods

Stratigraphic sections were measured with a Brunton compass and jacob staff, lithofacies described, and samples obtained for petrographic and geochronologic analyses at six locations (Fig. 2). The measured-section sites were selected to straddle the western margin of the Abiquiu embayment and the principal mapped intrabasinal faults (Kelley 1978; Moore 2000) across which Abiquiu Formation is exposed. Emphasis was placed on localities offering excellent outcrop exposure, although some sections have long covered intervals, especially at forested Cerro Pedernal. Closely spaced sections C and D form a nearly complete composite section within the same fault block, although each is partially covered.

Petrographic thin sections were prepared and point counted for 112 samples (data set in JSR’s digital archives, see Acknowledgments). Data reported by Smith (1995) from 25 additional samples collected at section E were included in the data analysis. Densely cemented horizons were avoid-

TABLE 1.—Summary of stream-profile-simulation results (LONGPRO)

Initial Water Discharge, m ³ /s	Initial Sediment Mass Feed Rate, kg/s	Change in Headwater Elevation, m	Change in Water Discharge, m ³ /s	Change in Sediment Mass Feed Rate, kg/s	Resulting Change in Bed Elevation at 90 km, m	Resulting Change in Bed Elevation at 160 km, m
10	0.5	500	—	—	+130	+40
10	0.5	2200	—	—	+140	+30
10	0.5	—	-5	+0.5	+300	+170
5	1.0	200	—	—	+40	+30
5	1.0	1300	—	—	+100	+80
10	0.5	1300	-5	+0.5	+430	+300

TABLE 2.—Summary of flexural-load-simulation results (CONTIN)

Rigidity (Nm)	Load	Deflection at Cerro Pedernal (m)	
		San Juan Volcanic Field Load	Latir Volcanic Field Load
10 ²²	volcanic field + volcanoclastic-apron	-287	-166
	volcanic field only	+12	+37
10 ²³	volcanic field + volcanoclastic-apron	-332	-271
	volcanic field only	+35	-60
10 ²⁴	volcanic field + volcanoclastic-apron	-404	-371
	volcanic field only	-121	-166

ed and most samples are poorly consolidated fine- to medium-grained sandstone. Thin sections were stained to facilitate identification of feldspars, and 300 points were counted on each slide using the Gazzi–Dickinson method (Ingersoll et al. 1984).

Point-count categories (Table 2) were selected to be sensitive to the mixed provenance of the Abiquiu Formation. Undulose-extinction quartz, microcline, and orthoclase are derived from nonvolcanic sources in the remnant Laramide uplifts or from Eocene and older sedimentary strata. Alkali-rhyolite-derived detritus includes abundant straight-extinction quartz, sanidine, and felsite rock fragments that are indicative of erosion of volcanic materials of the Latir volcanic field (Ingersoll and Cavazza 1991), because the dacitic tuffs of southeastern San Juan volcanic field contain very sparse sanidine and almost no quartz (Lipman 1975, 1989; Lipman et al. 1996). Ingersoll et al. (1990), Ingersoll and Cavazza (1991), and Smith (1995) mostly attributed quartz- and sanidine-poor volcanoclastic sediment rich in plagioclase and intermediate-composition rock fragments to sources in the San Juan volcanic field. Such a unique designation is problematic, however, because intermediate volcanism also characterized the Latir volcanic field mostly before but also after eruption of the Amalia Tuff (Lipman 1983; Lipman and Reed 1989).

Geochronological investigations were undertaken to corroborate stratigraphic correlations and provenance interpretations and to provide temporal control for tectonic activity suggested by stratigraphic-thickness variation. Eleven samples were analyzed by the ⁴⁰Ar/³⁹Ar method at the New Mexico Geochronology Research Laboratory. Sanidine crystals were separated from seven pumice and ignimbrite clasts in the upper member of the Abiquiu Formation. Two additional sanidine separates were prepared from samples of the distal outflow sheet of the Amalia Tuff (the tuff of Cañada del Agua of Manley and Wobus 1982b) in the southeastern Tusas Mountains. After irradiation, the isotopic ratios of 2–15 single sanidine crystals from each sample were analyzed following CO₂ laser fusion. Biotite and hornblende from four samples, three of which also contain sanidine, were analyzed by the resistance-furnace incremental heating method. Hornblende in two of these samples yielded disturbed spectra without age plateaus, and no ages were assigned to these hornblende separates. Separation and analytical methods are described in McIntosh and Chamberlin (1994) and data are available in McIntosh (2001) and summarized in Table 3.

Results

Lithostratigraphic Correlation.—Three distinct stratigraphic intervals designated by Smith (1995) at Arroyo del Cobre (section E) are readily correlated throughout the Abiquiu embayment from Cañones (section B) northeastward to Sierra Negra (section F; Figs. 2, 8). These lithostratigraphic divisions are made on the basis of contrasting relative abundances of sharply erosional lenticular channel deposits and poorly stratified, tabular pumice-lapilli-rich beds. Interval I of Smith (1995) consists of lenticular, pebbly sandstone channel facies with intervening tabular, tuffaceous fine sandstone and siltstone. Pebbles are mostly vesicular basalt and andesite, rare quartzite, and conspicuous pebbles and cobbles of white, highly porphyritic hornblende–biotite quartz latite, which are also abundant in the Cordito Member of the Los Pinos Formation. Interval II is characterized

TABLE 3.—Point-count categories.

Component (and Symbol)	Description
Quartz (<i>Q</i>)	
Quartz: undulose extinction or polycrystalline (<i>Q_u</i>)	Polycrystalline quartz grains and monocrystalline or polycrystalline quartz exhibiting undulose extinction.
Quartz: straight extinction (<i>Q_s</i>)	Monocrystalline quartz grains exhibiting complete optical extinction at a single position of the microscope stage; in some cases embayed and in some cases with one or more well preserved crystal faces
Feldspar (<i>F</i>)	
Sanidine (<i>F_s</i>)	Fresh, unaltered grains of alkali feldspar, untwinned or Carlsbad twin; some with slightly sweeping extinction
Microcline or Orthoclase (<i>F_i</i>)	Potassium feldspar, typically altered at grain boundary or in interior; microcline shows Carlsbad pericline twinning; orthoclase may or may not be Carlsbad-twinned
Plagioclase (<i>F_p</i>)	All feldspar lacking potassium-feldspar stain; in some cases radially zoned
Accessory Minerals	
Brown or green-brown amphibole (<i>A_{brn}</i>)	Amphibole with brown/red-brown or brown/green pleochroism; commonly rimmed or largely replaced by opaque minerals; primarily to exclusively oxyhornblende.
Blue-green amphibole (<i>A_{brn}</i>)	Amphibole with blue-green/green pleochroism.
Pyroxene (<i>Pyx</i>)	Orthopyroxene and clinopyroxene
Biotite (<i>Bio</i>)	
Muscovite (<i>Mus</i>)	
Opaque minerals (<i>Op</i>)	
Other nonopaque minerals (<i>Oth</i>)	
Lithic Fragments (<i>L</i>)	
Felsic volcanic lithic fragment (<i>L_v</i>)	Fragments composed of fine grained quartz and alkali feldspar in some instances with associated quartz or sanidine phenocrysts; devitrified lava or ignimbrite fragments
Volcanic glass (<i>L_{vg}</i>)	Glassy volcanic fragment; cuspat and pumiceous ash shards and small lapilli
Tuff (<i>L_t</i>)	Fragmental volcanic rock, typically with eutaxitic or axiolic texture; commonly contain other lithic fragments or crystals of sanidine, quartz, plagioclase, or biotite
Intermediate volcanic lithic fragment (<i>L_i</i>)	Fragments of volcanic-rock groundmass dominated by plagioclase microlites and interstitial pyroxene and opaque minerals; in some cases associated with phenocrysts of hornblende, pyroxene, and/or zoned plagioclase
Metamorphic lithic fragment (<i>L_m</i>)	Foliated polycrystalline-quartz and muscovite grain; foliated micaceous grains in some cases including blue-green amphibole
Sedimentary rock fragment (<i>L_s</i>)	Nonfoliated polycrystalline nonvolcanic rock fragments

by tabular, medium to thick bedded, massive to crudely stratified pumiceous sandstone with thin tuffaceous siltstone layers. The abundant pumice lapilli contain only quartz and sanidine characteristic of alkali-rhyolite ejecta from the Latir volcanic field (Lipman 1983; Ingersoll and Cavazza 1991). The upper half of interval II contains clasts of densely welded Amalia Tuff as large as 80 cm across (Smith 1995). Interval III consists of lenticular channel sandstone with basal-pebble-lag deposits interbedded with 1–3 m thick, thin-bedded fine sandstone and laminated mudstone and shale. In addition to pebbles of Amalia Tuff, interval III contains clasts of a distinctive orange, crystal-poor, lithic-rich, vapor-phase-lithified rhyolitic ignimbrite (Smith 1995).

Moore (2000) recognized additional stratigraphic intervals. Exposures below interval I of Smith (1995) at Arroyo del Cobre (section E) include 35 m of tabular and pumiceous strata without an exposed base. To maintain coherence with the terminology of Smith (1995), these strata are labeled as interval sub-I. Notably, the tabular, pumiceous beds of sub-I are not recognized at sections B and D, where the base of the upper member is exposed (Fig. 8). At Barranca (section D), interval III strata are overlain by interval IV, consisting of poorly sorted, tabular, pumiceous strata grading upward into pumice-rich strata with a greater abundance of lenticular channel-fill pebbly sandstone. Interval IV is also recognized at Cañones (section B) and Sierra Negra (section F). The upper parts of interval III and interval IV contain a variety of crystal-rich to crystal-poor, commonly biotite-bearing rhyolite-ignimbrite clasts with subordinate fragments of Amalia Tuff.

Compositional Variation.—Poor quality of exposure at Cerro Pedernal (section A, Figs. 2 and 8) inhibits recognition of intervals sub-I to IV as defined by facies character within the Abiquiu embayment, thus requiring

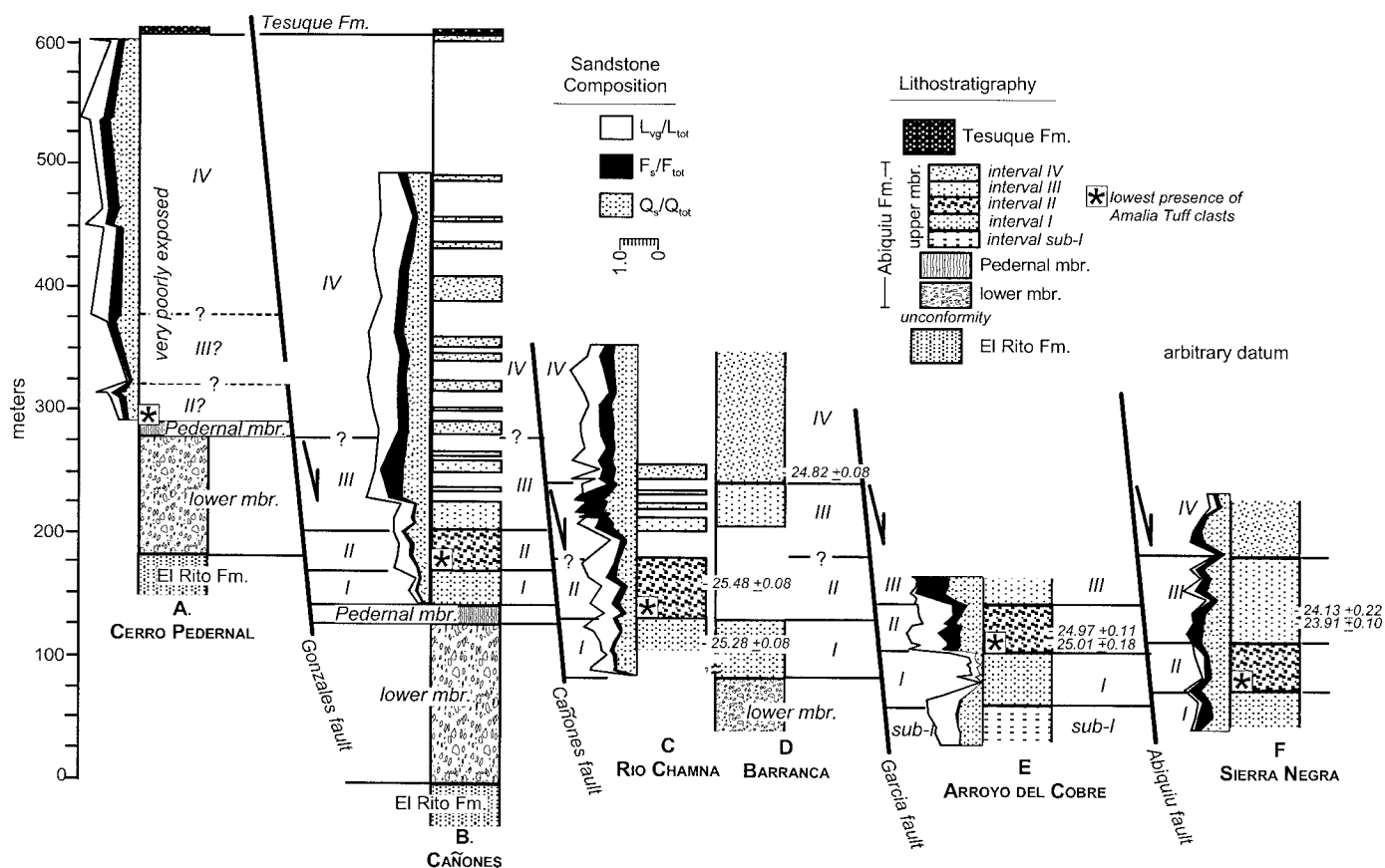


FIG. 8.—Stratigraphic correlations (arbitrary datum) for the Abiquiu Formation between Cerro Pedernal and the western Abiquiu embayment (locations of sections are labeled on Figure 2). Correlations within the embayment are based on stratigraphic intervals with distinctive lithofacies character. Selected sandstone-petrographic parameters are also illustrated and show the strongest relationship to lithofacies intervals at section E. Petrographic data are combined for sections C and D into a single column. Poor exposure at Cerro Pedernal prohibits correlation of lithofacies intervals, but sandstone composition, and presence of Amalia Tuff clasts at the base of the section, suggest correlation to intervals II and higher within the Abiquiu embayment.

consideration of compositional parameters for correlation. If intervals are compositionally distinct, as suggested by Smith (1995), then these intervals can be defined at Cerro Pedernal from petrographic data in the absence of sufficient exposure for direct correlation from measured-section descriptions.

The sandstone composition of intervals I–III are very distinct at Arroyo del Cobre (Smith 1995), but these distinctions are not as apparent when data from other sections in the Abiquiu embayment are included (Fig. 9). Although the lower abundance of sanidine and straight-extinction quartz in interval I and greater abundance of sanidine and generally less volcanic glass in interval III are characteristic of all sections, compositional fields overlap considerably (Fig. 9). Discriminant analysis, utilized by Ingersoll (1990) and Ingersoll and Cavazza (1991) to distinguish provenance in northern New Mexico, fails to distinguish the stratigraphic intervals. The along-strike changes in sandstone composition suggest laterally varying provenance. The strong inverse relationship between nonvolcanic potassium feldspar and straight-extinction quartz (Fig. 9A) suggests that most straight-extinction quartz is volcanic. Generally greater amounts of nonvolcanic feldspar and lesser straight-extinction quartz in sections east and west of Arroyo del Cobre may reflect greater tributary input from basement rocks exposed in the southeastern Tuzas Mountains and Sierra Nacimiento, respectively, which could account for most, if not all, of the lateral compositional variability. Overall, basement-rock contributions appear to decrease upsection (Fig. 9A). Although compositional characteristics of intervals overlap considerably, the general compositional traits remain apparent in the combined data from Abiquiu embayment sites (Fig. 10): in-

tervals II and IV contain the most glassy volcanic detritus; interval III contains the most sanidine whereas intervals sub I and I contain the least; interval I contains the most nonvolcanic feldspar and intermediate-composition-volcanic-lithic fragments.

Because of lateral compositional variation, the petrographic characteristics of the Cerro Pedernal section are compared to the next closest section at Cañones (section B) rather than to all of the Abiquiu embayment data (Fig. 11). Notably, cobbles of Amalia Tuff and other rhyolitic ignimbrites are found in the lowest exposures of the upper member at Cerro Pedernal. This is consistent with the abundance of sanidine in low exposures at Cerro Pedernal, which is higher than interval I at any section (Fig. 10A) and also generally greater than interval II at Cañones (Fig. 11B). Although the Cerro Pedernal section in general is impoverished in glassy lithic fragments compared to Cañones, it is most similar to intervals III and IV (Fig. 11).

Geochronology

$^{40}\text{Ar}/^{39}\text{Ar}$ analyses yielded high-quality ages for sanidine and mixed results for biotite and hornblende (Table 3). Of 90 sanidine crystals analyzed in nine samples, only five were discarded from final age calculations because of low radiogenic yield or anomalously old ages, thought to represent contaminant or xenocrystic crystals. Biotite incremental-heating age spectra yielded plateaus of variable quality and calculated on the basis of steps accounting for more than 80% of the ^{39}Ar released, with one exception. Hornblende in two samples yielded disturbed spectra without age plateaus, and no ages were assigned to these hornblende separates. The remaining

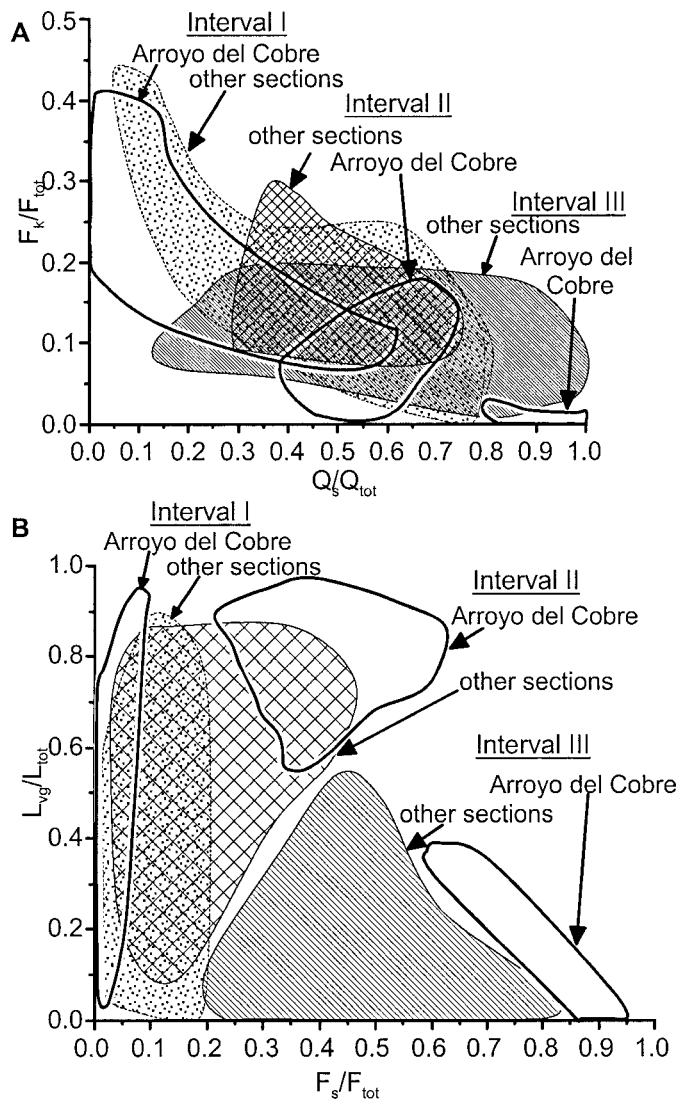


FIG. 9.—Comparison of upper member sandstone composition at the Arroyo del Cobre section (E, in Fig. 2) to other localities in the Abiquiu embayment. Although each interval is compositionally distinct at Arroyo del Cobre (Smith 1995) these distinctions are less apparent within the larger data set. **A**) The generally inverse relationship between the proportion of microcline and orthoclase to total feldspar and the proportion of quartz with straight, nonundulose extinction suggests that most straight-extinction quartz is of volcanic origin and that basement-rock contributions decrease up section. The proportion of basement-derived grains is more variable and generally greater at sections in the eastern and western embayment, which are closer to Precambrian outcrops, than in the central embayment at Arroyo del Cobre. **B**) Sanidine and volcanic-glass grains vary in abundance and allow for clear distinction of intervals I–III at Arroyo del Cobre. The greater abundance of basement-derived feldspars at other localities leads to generally lower sanidine/ F_{tot} than at Arroyo del Cobre.

hornblende age spectrum yielded a plateau age with 91.5% of the ^{39}Ar released, and that was consistent with ages obtained for biotite and sanidine extracted from the same sample.

Sanidine ages are interpreted to be most reliable for two reasons. First, the single-crystal laser-fusion method permits exclusion of contaminant and xenocrystic crystals and those with disturbed argon systematics, whereas such hornblende and biotite crystals cannot be excluded from the multi-crystal separates used in the resistance-furnace incremental-heating method. Second, hydrous minerals are not stable in the ultra-high vacuum extraction

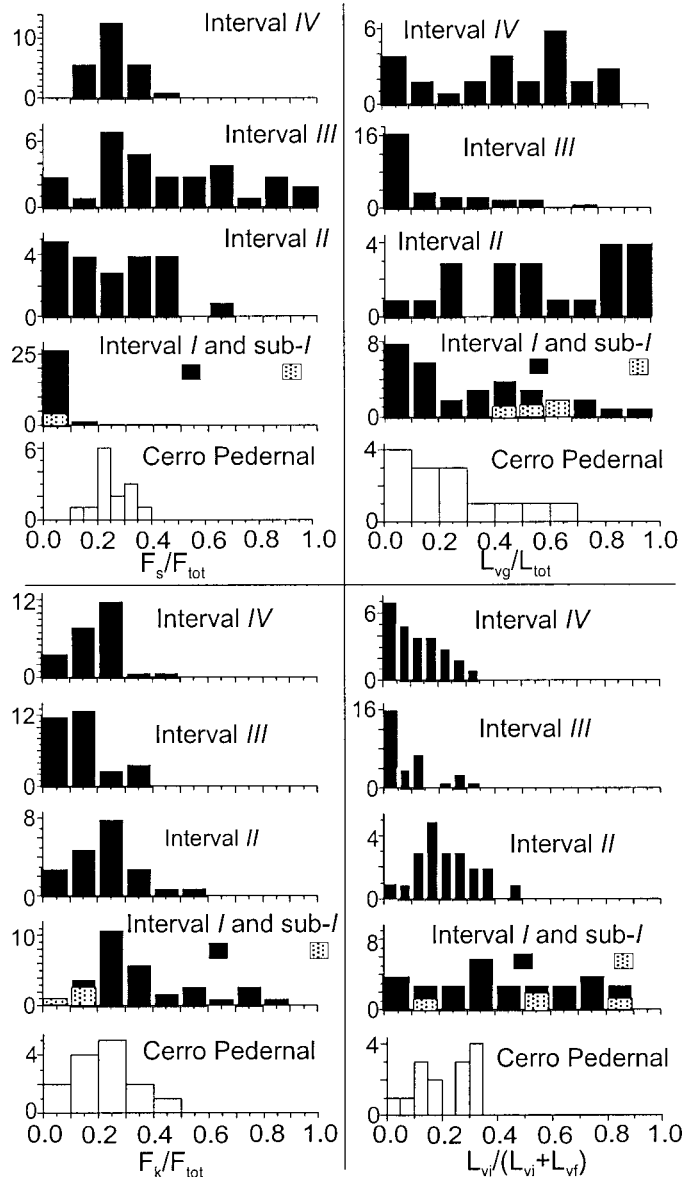


FIG. 10.—Histograms summarizing sandstone-compositional characteristics of stratigraphic intervals in the upper member of the Abiquiu Formation and comparison with the Cerro Pedernal section. Although composition ranges significantly within intervals, intervals II and IV are notable for generally higher abundance of volcanic-glass grains; interval III is notable for generally greater sanidine and intervals sub-I and I contain generally more nonvolcanic feldspar and more andesitic rock fragments. Cerro Pedernal samples are most like intervals II–IV (see Fig. 11).

system and can cause flat age spectra for biotite and hornblende separates when the actual argon distribution is much more complicated.

Ages of samples collected in the lower half of the upper member all fall in the narrow range between about 27 Ma and 24 Ma (Fig. 8, Table 4). For the most part, ages are progressively younger upsection, suggesting redeposition of pyroclastic detritus soon after eruption (Fig. 12). All dates are younger than the ignimbrites erupted in the southeastern San Juan volcanic field (Lipman et al. 1996).

Smith (1995) interpreted the massive beds of interval II to record widespread redeposition of readily eroded Amalia Tuff ignimbrite as debris flows, which is consistent with the first appearance of Amalia Tuff clasts in this interval. An age of 24.97 ± 0.11 Ma for single-crystal chatoyant sanidine separated from one of these clasts is indistinguishable from the

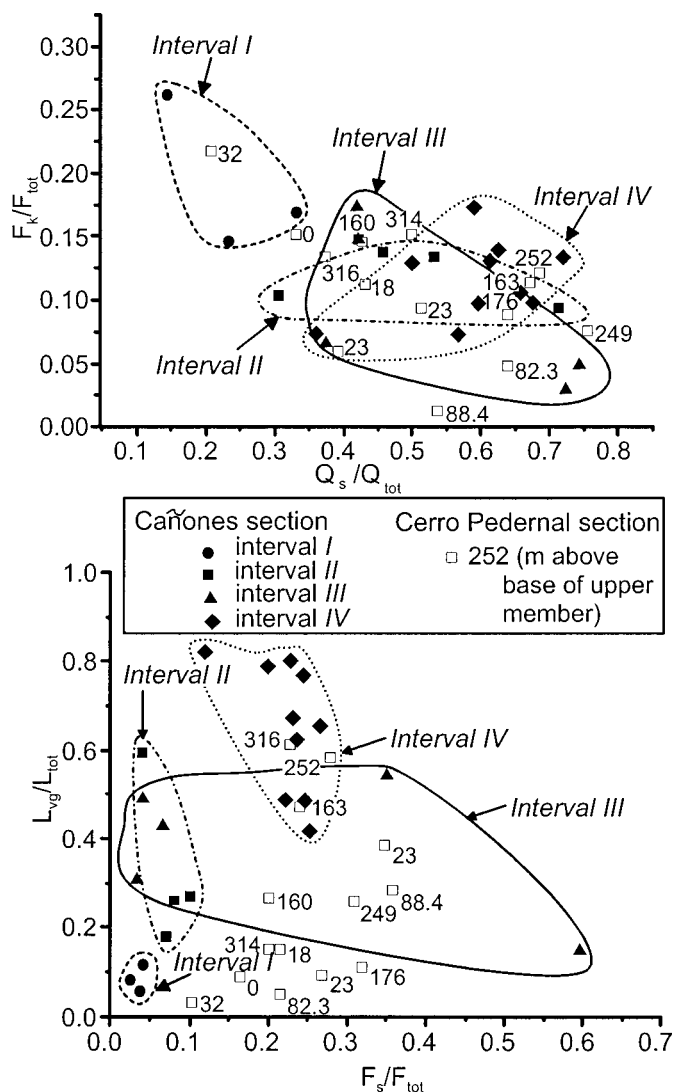


FIG. 11.—Comparison of most diagnostic (Fig. 9) sandstone-composition parameters for Cerro Pedernal and Cañones, the closest locality to Cerro Pedernal within the Abiquiu embayment. Two samples low in the Cerro Pedernal section (at 0 and 32 m above the base of the upper member) have low nonvolcanic feldspar and quartz contents comparable to interval I at Cañones, but intervening samples (at 18 and 23 m) are unlike interval I. Sanidine is also more abundant at the base of the Cerro Pedernal section than in interval I at Cañones, and nearly all samples from Cerro Pedernal contain a greater proportion of sanidine to total feldspar than in interval II at Cañones. These data suggest correlation of the Cerro Pedernal section to intervals III and IV, possibly in part to interval II, but not at all to interval I at Cañones.

25.01 ± 0.18 Ma age for pumice lapilli near the base of interval II. Because these dates are slightly younger than the 25.5 ± 0.1 and 25.7 ± 0.1 Ma $^{40}\text{Ar}/^{39}\text{Ar}$ ages for a multiple-crystal sanidine separate from the Amalia Tuff reported by Czamanske et al. (1990) we undertook single-crystal sanidine analyses of two samples from this tuff in the Tusas Mountains and obtained results of 25.06 ± 0.07 and 25.10 ± 0.07 Ma (Table 3). We prefer these results to those of Czamanske et al. (1990) because bulk mineral separates can include xenocrysts that skew results to an older age. Our new results for the Amalia Tuff support the correlation of pumiceous interval II to the time of eruption of the ignimbrite (Fig. 12). Two of three ages obtained for pumice in interval I are older than the Amalia Tuff as expected. The one disparate, younger age of 24.42 ± 0.18 Ma in interval I is for a biotite separate, which is not considered as reliable as the high-

precision sanidine age determinations. The single-crystal sanidine age of 25.28 ± 0.08 Ma from low in interval I in section C is probably the best estimate of the age of deposition of this interval (Fig. 12). Intervals III and IV contain dated pumice and tuff clasts derived from post-Amalia Tuff ignimbrites—with ages between 24 Ma and 25 Ma.

Synthesis.—The upper member of the Abiquiu Formation is divided into correlative intervals on the basis of facies character and, secondarily, by conglomerate-clast and sandstone composition. These correlations demonstrate stratal thickening across faults within and at the western margin of the Abiquiu embayment (Fig. 8). Intervals sub-I and I are clearly absent at Cerro Pedernal, and the presence of interval II cannot be conclusively demonstrated. Interval I is present at the next section to the northeast (Cañones, section B, Fig. 8), and the post-interval I section at Cañones is more than 400 m thick, compared to a total upper member thickness of 316 m at Cerro Pedernal. Interval sub-I is recognized only at Arroyo del Cobre and is not present at sections in fault blocks farther west. Even if one argued that interval sub-I is not well defined because of its presence in only one section, the pre-interval II section is only 27 m thick at Cañones compared to > 46 m at Barranca and > 75 m at Arroyo del Cobre. Interval II is close to the same thickness throughout the Abiquiu embayment. Interval III is about 40–50 m thick at sections between the Gonzales and Garcia faults but is 75 m thick farther east at Sierra Negra. These thickness variations imply down-to-the-east motion on the Gonzales, Cañones, and Garcia faults during deposition of the upper member of the Abiquiu Formation. The lack of thickness variability within interval II may reflect its rapid deposition across the entire area immediately following eruption of the Amalia Tuff rather than a significant hiatus in fault motion.

Stratigraphic relationships in the lower and Pedernal chert members also imply syndepositional faulting (Fig. 8). The combined thickness of these members is 108 m at Cerro Pedernal but increases abruptly to 162 m at Cañones. The Abiquiu Formation rests upon Eocene El Rito Formation at both sections with no evidence of a significant erosional disconformity to account for local thickness changes of this magnitude. The base of the lower member is not exposed east of the Cañones fault, so further basinward thickening cannot be unequivocally demonstrated. The origin of the calcareous, chalcedony-cemented layers of the Pedernal chert member is not clear, but pedogenic processes are consistent with geochemical profiles comparable to a soil-weathering profile (Vazzana 1980) and the petrographic similarity of the Pedernal chert horizons (Moore 2000) with silicified calcare in Kuwait (Khalaf 1988). If this paleosols interpretation is true, then the isolation of the Pedernal chert member in locations west of the Cañones fault may record pedogenesis during limited deposition west of the Abiquiu embayment contemporaneous with largely rift-restricted sedimentation east of the Cañones fault.

Geochronological data provide insights into the timing of faulting, but the lack of dateable horizons in the lower member does not permit determination of the earliest deformation. At least 75 m of section at Arroyo del Cobre, below interval II, is not represented at Cerro Pedernal, suggesting at least 75 m of differential subsidence across the intervening faults during deposition of intervals sub-I and I. At least 40 m of this displacement is estimated to have occurred between 25.28 ± 0.08 Ma, the best available date for interval I, and 25.08 ± 0.08 Ma, the average of two ages obtained for the Amalia Tuff. Thickening of the lower member between Cerro Pedernal and Cañones implies earlier motion of the Gonzales fault. The age of the lower member can be only broadly determined, however. Regional stratigraphic relations (Fig. 3) imply that the lower member and correlative Ritito Conglomerate are equivalent to volcanic and volcanoclastic rocks north of the Tusas Mountains as old as 30–35 Ma. However, the presence of an altered basalt flow low in the Ritito Conglomerate on the south flank of the Tusas Mountains (Smith 1938; Bingler 1968) suggests an age ≤ 27 Ma because no K–Ar dates on basalts in the region are older than 27 Ma (Baldrige et al. 1980; May 1980). These indirect age inferences are consistent with initial faulting along the western margin of the

TABLE 4.—Summary of $^{40}\text{Ar}/^{39}\text{Ar}$ age determinations. Data reported in McIntosh (2001)

Sample	Lat./Long.	Stratigraphic Position—Location			Sample Type	Sanidine ²		Biotite/Hornblende ³		
		Section	Interval	Height ¹		<i>n</i>	Age (Ma)	Steps	% ³⁹ Ar	Age (Ma)
8jm0617d	36.218 N 106.387 W	D	I	0 m	pumice lapilli			8	92%	24.42 ± 0.18 (bio)
8jm0706a	36.209 N 106.408 W	C	I	0 m	pumice lapilli	4	25.28 ± 0.08	3	37%	26.84 ± 0.30 (bio)
8jm0706n	36.208 N 106.387 W	C	II	58.5 m	pumice lapilli	9 (1)	25.48 ± 0.08	9	90%	25.94 ± 0.26 (bio)
AdC2	36.218 N 106.337 W	E	II	75 m	pumice lapilli	8 (2)	25.01 ± 0.18	6	91.5%	25.91 ± 0.22 (hb)
Abq59427x	36.216 N 106.337 W	E	II	80 m	ignimbrite clast (Amalia Tuff)	15	24.97 ± 0.11			
R980808b1	36.252 N 106.248 W	F	III	84.5 m	ignimbrite clast	6	23.91 ± 0.10			
R980808c1	36.252 N 106.248 W	F	III	93 m	ignimbrite clast	2	24.13 ± 0.22	7	88%	24.53 ± 0.10 (bio)
8jm0618i	36.213 N 106.388 W	D	IV	162 m	pumice lapilli	12 (1)	24.82 ± 0.08			
GS001	36.598 N 106.009 W	Cañada del Agua, NE of Las Tablas, NM (Amalia Tuff)			pumice lapilli	14 (1)	25.06 ± 0.07			
GS002	36.598 N 106.009 W	Cañada del Agua, NE of Las Tablas, NM (Amalia Tuff)			crystal-rich tuff	15	25.10 ± 0.07			

¹ Height above base of upper member.

² Single-crystal, laser total fusion age determinations; *n* = number of crystals analyzed (number of single-crystal ages discarded from age calculation).

³ Resistance-furnace incremental-heating age spectrum ages showing number of steps defining the plateau age and the percent of the total released ³⁹Ar in those steps.

Abiquiu embayment more or less coincident with the initial tilting of the San Luis basin in southern Colorado between 28 and 27 Ma (Lipman and Mehnert 1975).

The volcanoclastic component of the Abiquiu Formation is overwhelmingly, if not entirely, derived from the Latir volcanic field, corroborating correlations of Bingler (1968) and Manley (1981) to the Cordito Member of the Los Pinos Formation (Fig. 3). Suggestions that nearly all (Smith 1938; Ingersoll and Cavazza 1991; Ingersoll et al. 1990) or the lower part (Smith 1995) of the upper member could correlate to the San Juan–derived Esquibel Member of the Los Pinos Formation are contradicted by two

observations. First, sanidine, while not abundant, constitutes as much as 10% of total feldspar in interval sub-I and 40% in interval I samples and is inconsistent with the rarity of sanidine among tuff and lava erupted in the southeastern San Juan volcanic field (Lipman 1975, 1989). Second, all $^{40}\text{Ar}/^{39}\text{Ar}$ dates on pumice lapilli and tuff clasts, including those from interval I, post-date explosive eruptive activity in the southeastern San Juan Mountains and coincide with the time of known volcanism in the Latir volcanic field (Lipman 1983; Johnson et al. 1989). The abundance of intermediate-composition volcanic detritus in the lower part of the upper member (Fig. 9) more likely represents erosion from pre-Amalia Tuff lava flows in the Latir volcanic field (Lipman 1983; Lipman and Reed 1989) than from the San Juan volcanic field (cf., Ingersoll and Cavazza 1991; Smith 1995). These relationships imply that remnant Laramide topography in the southern Tusas Mountains was a barrier to the delivery of volcanoclastic detritus into the Abiquiu embayment until shortly before eruption of the Amalia Tuff. Erosion of pyroclastic debris from the Amalia Tuff and later ignimbrites erupted in the Latir field led to deposition of a widespread volcanoclastic apron that buried most of the southern Tusas Mountains, inundated the Abiquiu embayment, and was also deposited across most or all of the Sierra Nacimiento. This widespread dispersal of mostly rhyolitic volcanoclastic detritus to bury preexisting Laramide uplifts is reflected not only by erosional remnants of the volcanoclastic succession atop both Laramide mountain ranges (Fig. 1) but also the upward decrease in basement-derived detritus in the upper Abiquiu Formation (Figs. 9, 10).

INTEGRATED CONCLUSIONS

Both competing hypotheses for the roles of volcanism and rift-basin subsidence in accounting for Oligocene–early Miocene sedimentation in the Abiquiu embayment region pass crucial tests. Lateral correlation of stratigraphy within the Abiquiu Formation demonstrates syndepositional thickening across mapped faults into the Rio Grande rift within the same time frame as has been suggested for regional initiation of extension by other workers. Notably, this subsidence is remote from active volcanic centers where local strain might be argued (cf. Large and Ingersoll 1997). Rift subsidence was insufficient, however, to contain volcanoclastic aprons, particularly from the Latir volcanic field, which extended beyond the incipient rift basins and buried remnant topographic highs remaining from the Laramide orogeny. Aggradation beyond the demonstrated extent of subsidence along rift-related faults implies that volcanism-driven deposition

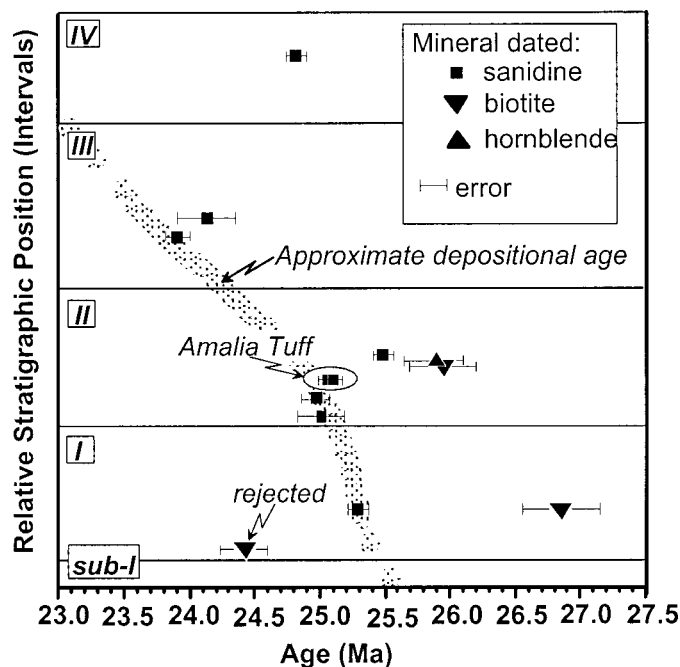


FIG. 12.—Graph depicting relative stratigraphic position of $^{40}\text{Ar}/^{39}\text{Ar}$ dates obtained from the upper Abiquiu Formation. Dates for Amalia Tuff in the Tusas Mountains are shown for comparison to dates from interval II. Note the greater precision of the sanidine age determinations and the generally younger ages at successively higher stratigraphic levels.

occurred. Overlap of the basin-bounding faults by volcanoclastic debris permits application of stratigraphic analysis to detect syndepositional faulting, and the volcanogenic material permits acquisition of geochronological data to constrain the time of faulting.

First-order computational simulations, though admittedly simplified and not well conditioned by input data, suggest that one or more consequences of volcanic activity are capable of explaining the deposition of the Abiquiu Formation beyond incipient subsiding rift basins and may have enhanced deposition within the basins. Although speculative, increasing headwater elevations and synvolcanic sediment loads may account for some component of upper Abiquiu deposition, but the simulations do not support accumulation of the total thickness of strata that are preserved (cf. Ingersoll et al. 1990). We suggest that regional flexural compensation of the mass of growing volcanic fields may be the most reasonable explanation for widespread deposition and preservation of the Abiquiu Formation beyond the nascent rift by producing a broad, shallow circumferential trough within which sediment accumulated. We cannot rule out the possibility that activation of steep faults at this time was partly caused by this load rather than entirely by tensional stress.

Flexural subsidence may account for widespread deposition of the lower and Pederal chert members of the Abiquiu Formation despite the paucity of volcanic detritus in these strata. The flexural moat of the San Juan volcanic field is postulated to have extended more than 200 km to the south. Detritus eroded from the volcanic field did not come into the Abiquiu embayment—Sierra Nacimiento area, however, because of the intervening barrier of the Tusas Mountains. Instead, the distal flexural moat was filled with sediment eroded from Precambrian-rock highlands until the Latir volcanoclastic apron surmounted the Tusas Mountains barrier (Fig. 3), whereupon debris eroded from the Amalia Tuff and younger ignimbrites was spread across the Tusas Mountains, Abiquiu embayment, Colorado Plateau, and Sierra Nacimiento.

This study of the Abiquiu Formation illustrates that volcanoclastic strata provide important insights into paleotectonic reconstructions. Abrupt changes in facies character, sediment composition, or both permit definition of stratigraphic intervals that can be correlated widely and used to examine evidence for syndepositional faulting and basin subsidence. Volcanism may indirectly cause sedimentation independently of regional basin tectonics. The volcanism-related mechanisms examined by us to account for accommodation of modest thickness of sedimentary strata require more refinement and testing but should not be ruled out when evaluating the stratigraphy of basins that include volcanoclastic-sediment fill.

ACKNOWLEDGMENTS

Partial financial support for this research was provided by Vastar Resources, Inc. and grants to Moore from the Geological Society of America, Rocky Mountain section of SEPM (Society for Sedimentary Geology), the New Mexico Geological Society, and Sigma Xi, The American Research Society. Valuable reviews by Colin North, Allard Martinus, and Niels Hovius improved the manuscript as did careful editing by John Southard. The petrographic data described in this paper have been archived, and are available in digital form, at the World Data Center-A for Marine Geology and Geophysics, NOAA/NGDC, 325 Broadway, Boulder, CO 80303; phone: 303-497-6339; fax: 303-497-6513; E-mail: wdcamgg@ngdc.noaa.gov; URL: <http://www.ngdc.noaa.gov/mgg/sepm/archive.index.html>.

REFERENCES

AHRENS, T.J., 1995, Rock physics and phase relations: A handbook of physical constants: American Geophysical Union, Reference Shelf, n. 3, 270 p.
BALDRIDGE, W.S., DAMON, P.E., SHAFIQUILLAH, M., AND BRIDWELL, R.J., 1980, Evolution of the central Rio Grande rift, New Mexico: new potassium-argon dates: Earth and Planetary Science Letters, v. 51, p. 309–321.
BALDRIDGE, W.S., FERGUSON, J.F., BRAILE, L.W., WANG, B., ECKHARDT, K., EVANS, D., SCHULTZ, C., GILPIN, B., JURACEK, G.R., AND BIEHLER, S., 1994, The western boundary of the Rio Grande rift in northern New Mexico: an aborted boundary?: Geological Society of America, Bulletin, v. 105, p. 1538–1558.

BALTZ, E.H., 1978, Resume of Rio Grande depression in north-central New Mexico: New Mexico Bureau of Mines and Mineral Resources, Circular 163, p. 210–228.
BAUER, P.W., JOHNSON, P.S., AND KELSON, K.I., 1999, Geology and hydrogeology of the southern Taos Valley, Taos County, New Mexico: Final Technical Report, Office of the State Engineer, 41 p.
BARKER, F., 1958, Precambrian and Tertiary geology of the Las Tablas quadrangle, New Mexico: New Mexico Bureau of Mines and Mineral Resources, Bulletin 45, 104 p.
BINGLER, E.C., 1965, Precambrian geology of the La Madera quadrangle, Rio Arriba County, New Mexico: New Mexico Bureau of Mines and Mineral Resources, Bulletin 80, 132 p.
BINGLER, E.C., 1968, Geology and mineral resources of Rio Arriba County, New Mexico: New Mexico Bureau of Mines and Mineral Resources, Bulletin 91, 158 p.
BLUM, M.D., AND TÖRNQVIST, T.E., 2000, Fluvial responses to climate and sea level change: A review and a look forward: Sedimentology, v. 47, supplement 1, p. 2–48.
BRISTER, B.S., AND GRIES, R.R., 1994, Tertiary stratigraphy and tectonic development of the Alamosa basin (northern San Luis basin), Rio Grande rift, south-central Colorado, in Keller, G.R., and Cather, S.M., eds., Basins of the Rio Grande Rift: Structure, Stratigraphy, and Tectonic Setting: Geological Society of America, Special Paper 291, p. 39–58.
BUTLER, A.P., JR., 1971, Tertiary volcanic stratigraphy of the eastern Tusas Mountains, southwest of the San Luis valley, Colorado—New Mexico: New Mexico Geological Society, Guidebook 22, p. 289–300.
CHAPIN, C.E., 1988, Axial basins of the northern and central Rio Grande rift in Sloss, L.L., ed., Sedimentary cover—North American craton: U.S. Geological Society of America, The Geology of North America, v. D-2, p. 165–170.
CHAPIN, C.E., AND CATHER, S.M., 1994, Tectonic setting of the axial basins of the northern and central Rio Grande rift, in Keller, G.R., and Cather, S.M., eds., Basins of the Rio Grande Rift: Structure, Stratigraphy, and Tectonic Setting: Geological Society of America, Special Paper 291, p. 5–26.
CZAMANSKE, G.K., FOLAND, K.A., KUBACHER, F.A., AND ALLEN, J.C., 1990, The ⁴⁰Ar/³⁹Ar chronology of caldera formation, intrusive activity and Mo-ore deposition near Questa, New Mexico: New Mexico Geological Society, Guidebook 41, p. 355–358.
DONEY, H.H., 1968, Geology of the Cebolla quadrangle, Rio Arriba County, New Mexico: New Mexico Bureau of Mines and Mineral Resources, Bulletin 92, 114 p.
EKAS, L.M., INGERSOLL, R.V., BALDRIDGE, W.S., AND SHAFIQUILLAH, M., 1984, The Chama—El Rito Formation, Española basin, New Mexico: New Mexico Geological Society, Guidebook 35, p. 137–143.
INGERSOLL, R.V., BULLARD, T.F., FORD, R.L., GRIMM, J.P., PICKLE, J.D., AND SARES, S.W., 1984, The effect of grain size on detrital modes; a test of the Gazzi—Dickinson point-counting method: Journal of Sedimentary Petrology, v. 54, p. 103–116.
INGERSOLL, R.V., 1990, Actualistic sandstone petrofacies: discriminating modern and ancient source rocks: Geology, v. 18, p. 733–736.
INGERSOLL, R.V., AND CAVAZZA, W., 1991, Reconstruction of Oligo—Miocene volcanoclastic dispersal patterns in north-central New Mexico using sandstone petrofacies, in Fisher, R.V., and Smith, G.A., eds., Sedimentation in Volcanic Settings: SEPM, Special Publication 45, p. 227–236.
INGERSOLL, R.V., CAVAZZA, W., BALDRIDGE, W.S., AND SHAFIQUILLAH, M., 1990, Cenozoic sedimentation and paleotectonics of north-central New Mexico: implications for initiation and evolution of the Rio Grande rift: Geological Society of America, Bulletin, v. 102, p. 1288–1296.
JOHNSON, C.M., CZAMANSKE, G.K., AND LIPMAN, P.W., 1989, Geochemistry of intrusive rocks associated with the Latir volcanic field, New Mexico, and contrast between evolution of plutonic and volcanic rocks: Contributions to Mineralogy and Petrology, v. 103, p. 90–109.
JORDAN, T.E., 1981, Thrust loads and foreland basin evolution, Cretaceous, western United States: American Association of Petroleum Geologists, Bulletin, v. 65, p. 2506–2520.
KARLSTROM, K.E., CATHER, S.M., KELLEY, S.A., HEIZLER, M.T., PAZZAGLIA, F.J., AND ROY, M., 1999, Sandia Mountains and Rio Grande rift, New Mexico: Ancestry of structures and history of deformation: New Mexico Geological Society, Guidebook 50, p. 155–166.
KELLEY, V.C., 1978, Geology of the Española Basin, New Mexico: New Mexico Bureau of Mines and Mineral Resources, Geologic Map 48, scale 1:250,000.
KHALAF, F.I., 1988, Petrography and diagenesis of silcrete from Kuwait, Arabian Gulf: Journal of Sedimentary Petrology, v. 58, p. 1014–1022.
LARGE, E., AND INGERSOLL, R.V., 1997, Miocene and Pliocene sandstone petrofacies of the northern Albuquerque basin, New Mexico, and implications for evolution of the Rio Grande rift: Journal of Sedimentary Research, v. 67, p. 462–468.
LIPMAN, P.W., 1975, Evolution of the Platoro caldera complex and related volcanic rocks, southeastern San Juan Mountains, Colorado: U.S. Geological Survey, Professional Paper 852, 128 p.
LIPMAN, P.W., 1983, The Miocene Questa caldera, northern New Mexico: relation to batholith emplacement and associated molybdenum mineralization: Proceedings of the Denver Regional Exploration Geologists Society, Symposium, p. 133–147.
LIPMAN, P.W., COMPILER, 1989, Excursion 16B: Oligocene—Miocene San Juan volcanic field, Colorado: New Mexico Bureau of Mines and Mineral Resources, Memoir 46, p. 303–380.
LIPMAN, P.W., DUNGAN, M.A., BROWN, L.L., AND DEINO, A., 1996, Recurrent eruption and subsidence at the Platoro caldera complex, southeastern San Juan volcanic field, Colorado: New tales from old tuff: Geological Society of America, Bulletin, v. 108, p. 1039–1055.
LIPMAN, P.W., AND MEHNERT, H.H., 1975, Late Cenozoic basaltic volcanism and development of the Rio Grande depression in the southern Rocky Mountains, in Curtis, B.F., ed., Cenozoic History of the Southern Rocky Mountains: Geological Society of America, Memoir 144, p. 119–154.
LIPMAN, P.W., AND MEHNERT, H.H., 1979, The Taos Plateau volcanic field, northern Rio Grande rift, New Mexico, in Riecker, R.E., ed., Rio Grande Rift: Tectonics and Magmatism: Washington, American Geophysical Union, p. 280–311.
LIPMAN, P.W., AND REED, J.C., JR., 1989, Geologic map of the Latir volcanic field and adjacent

- areas, northern New Mexico: U.S. Geological Survey, Miscellaneous Investigations Series, Map I-1907, scale 1:48,000.
- MANLEY, K., 1981, Redefinition and description of the Los Pinos Formation of north-central New Mexico: Geological Society of America, Bulletin, part 1, v. 92, p. 984–989.
- MANLEY, K., AND WOBUS, R.A., 1982a, Reconnaissance geologic map of the Mule Canyon quadrangle, Rio Arriba County, New Mexico: U.S. Geological Survey, Miscellaneous Field Studies, Map MF-1407, scale 1:24,000.
- MANLEY, K., AND WOBUS, R.A., 1982b, Reconnaissance geologic map of the Las Tablas quadrangle, Rio Arriba County, New Mexico: U.S. Geological Survey, Miscellaneous Field Studies, Map MF-1408, scale 1:24,000.
- MAY, S.J., 1980, Neogene geology of the Ojo Caliente–Rio Chama area, Española basin, New Mexico [unpublished Ph.D. thesis]: Albuquerque, University of New Mexico, 204 p.
- MENARD, H.W., 1964, Marine Geology of the Pacific: New York, McGraw Hill, 271 p.
- MCINTOSH, W.C., 2001, $^{40}\text{Ar}/^{39}\text{Ar}$ geochronology results from the Abiquiu Formation, New Mexico, in McIntosh, W.C., and Heizler, M.T., eds., $^{40}\text{Ar}/^{39}\text{Ar}$ Geochronology Data Files and Reports: New Mexico Bureau of Geology and Mineral Resources, Open File Report 500, Ar-11, 6 p.
- MCINTOSH, W.C., AND CHAMBERLIN, R.M., 1994, $^{40}\text{Ar}/^{39}\text{Ar}$ geochronology of middle to late Cenozoic ignimbrites, mafic lavas, and volcanoclastic rocks in the Quemado region, New Mexico: New Mexico Geological Society, Field Conference, Guidebook 45, p. 165–185.
- MOORE, J.D., 2000, Tectonics and volcanism during deposition of the Oligocene–lower Miocene Abiquiu Formation in northern New Mexico [unpublished M.S. thesis]: Albuquerque, University of New Mexico, 147 p.
- MORGAN, P., AND GOLOMBEK, M.P., 1984, Factors controlling the phases and styles of extension in the northern Rio Grande rift: New Mexico Geological Society, Guidebook 35, p. 13–20.
- MUEHLBERGER, W.R., 1967, Geology of the Chama quadrangle: New Mexico Bureau of Mines and Mineral Resources, Bulletin 89, 114 p.
- MUEHLBERGER, W.R., 1968, Geology of the Brazos Peak quadrangle, New Mexico: New Mexico Bureau of Mines and Mineral Resources, Geologic Map 22, scale 1:48,000 + 7 p. text.
- SLINGERLAND, R., HARBAUGH, J.W., AND FURLONG, K., 1994, Simulating Clastic Sedimentary Basins: Englewood Cliffs, New Jersey, Prentice Hall, 220 p.
- SMITH, G.A., 1987, Sedimentology of volcanism-induced aggradation in fluvial basins: Examples from the Pacific Northwest, U.S.A., in Ethridge, F., Flores, R., and Harvey, M., eds., Recent Developments in Fluvial Sedimentology: SEPM, Special Publication 39, p. 217–229.
- SMITH, G.A., 1991, Facies sequences and geometries in continental volcanoclastic sediments, in Fisher, R.V. and Smith, G.A., eds., Sedimentation in Volcanic Settings: SEPM, Special Publication 45, p. 109–122.
- SMITH, G.A., 1995, Paleogeographic, volcanologic and tectonic significance of the upper Abiquiu Formation at Arroyo del Cobre, New Mexico: New Mexico Geological Society, Guidebook 46, p. 261–270.
- SMITH, G.A., 2000, Oligocene onset of Santa Fe Group sedimentation near Santa Fe, New Mexico (abstract): New Mexico Geology, v. 22, p. 43.
- SMITH, G.A., in press, Middle to late Cenozoic development of the Rio Grande rift and adjacent regions in northern New Mexico, in Mack G., and Giles, K., eds., Geology of New Mexico, v. 1: New Mexico Geological Society, Special Publication.
- SMITH, G.A., AND LANDIS, C.A., 1995, Intra-arc basins, in Busby, C., and Ingersoll, R.V., eds., Tectonics of Sedimentary Basins: London, Blackwell, p. 263–298.
- SMITH, G.A., VINCENT, K.R., AND SNEE, L.W., 1989, An isostatic model for basin formation in and adjacent to the central Oregon High Cascade Range, in Muffler, L.P.J., Weaver, C., and Blackwell, D., eds., Geological, Geophysical, and Tectonic Setting of the Cascade Range: U.S. Geological Survey, Open-File Report 89-178, p. 411–428.
- SMITH, H.T.U., 1938, Tertiary geology of the Abiquiu quadrangle, New Mexico: Journal of Geology, v. 46, p. 933–965.
- STEVEN, T.A., LIPMAN, P.W., HAIL, W.D., BARKER, F., AND LUEDKE, R.G., 1974, Geologic map of the Durango quadrangle, southwestern Colorado: U.S. Geological Survey, Miscellaneous Field Investigation, Map I-764, scale 1:250,000.
- TIMMER, R.S., 1976, Geology and sedimentary copper deposits in the western part of the Jarosa and Seven Springs quadrangles, Rio Arriba and Sandoval Counties, New Mexico [unpublished M.S. thesis]: Albuquerque, University of New Mexico, 151 p.
- VAZZANA, M.E., 1980, Stratigraphy, sedimentary petrology and basin analysis of the Abiquiu Formation (Oligo–Miocene), north-central New Mexico [unpublished M.S. thesis]: Albuquerque, University of New Mexico, 115 p.
- VAZZANA, M.E., AND INGERSOLL, R.V., 1981, Stratigraphy, sedimentary petrology and basin analysis of the Abiquiu Formation (Oligo–Miocene), north-central New Mexico: Geological Society of America, Bulletin, v. 92, pt. 1, p. 990–992.
- WATTS, A.B., 1978, An analysis of isostasy in the world's oceans, part I. Hawaiian–Emperor seamount chain: Journal of Geophysical Research, v. 75, p. 3941–3954.
- WOBUS, R.A., AND MANLEY, K., 1982, Reconnaissance geologic map of the Burned Mountain quadrangle, Rio Arriba County, New Mexico: U.S. Geological Survey, Miscellaneous Field Studies, Map MF-1409, scale 1:24,000.

Received 21 September 2001; accepted 6 May 2002.